Journal of Hazardous Materials 258–259 (2013) 19–26

Contents lists available at SciVerse ScienceDirect

Journal of Hazardous Materials

journal homepage: www.elsevier.com/locate/jhazmat

Preparation and characterization of TiO_2/HZSM-11 zeolite for photodegradation of dichlorvos in aqueous solution

Silvina Gomez[a], Candelaria Leal Marchena[a], Luis Pizzio[b,**], Liliana Pierella[a,*]

[a] Grupo Zeolitas, CITeQ (Centro de Investigación y Tecnología Química), Facultad Córdoba, Universidad Tecnológica Nacional, Maestro López esq. Cruz Roja Argentina, Córdoba, Argentina

[b] Centro de Investigación y Desarrollo en Ciencias Aplicadas "Dr. J. J. Ronco" (CINDECA), Departamento de Química, Facultad de Ciencias Exactas, UNLP-CCT La Plata, 47 Nº. 257, 1900 La Plata, Buenos Aires, Argentina

HIGHLIGHTS

- TiO_2/HZMS-11(30%) sample degraded efficiently aqueous solutions of dichlorvos.
- TiO_2/HZSM-11 samples did not show evidence of rutile phase.
- HZMS-11 (support) is not active by itself in the degradation of dichlorvos.
- The catalyst can be reused without activity loss during at least four cycles.

GRAPHICAL ABSTRACT

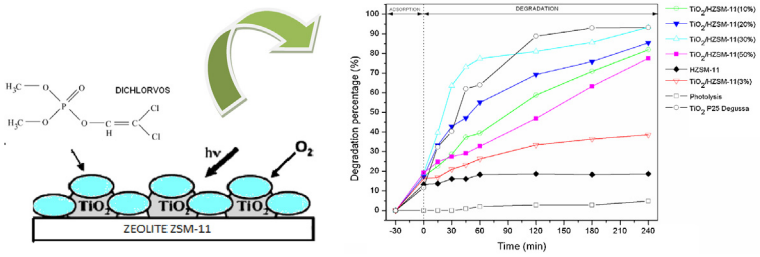

ARTICLE INFO

Article history:
Received 20 January 2013
Received in revised form 19 April 2013
Accepted 21 April 2013
Available online xxx

Keywords:
Dichlorvos
Water treatment
Photodegradation
TiO_2/Zeolite
Characterization

ABSTRACT

The TiO_2/HZSM-11 materials were synthesized using titanium isopropoxide as a TiO_2 precursor and HZSM-11 a medium pore size zeolite with high thermal and chemical resistance as support. The amount of titanium isopropoxide was varied in order to obtain TiO_2 concentrations of 3, 10, 20, 30 and 50 wt% in the final material. They were characterized by a series of complementary techniques: X-ray diffraction (XRD), ultraviolet–visible diffuse reflectance spectroscopy (DRS), transmittance Fourier transform infrared spectroscopy (FTIR) and scanning electron microscopy (SEM). The surface area of the TiO_2/HZSM-11 samples decreased with the increment of TiO_2 loading. As result of the increment of the calcination temperature from 450 to 800 °C an increase in the size of the anatase crystals was observed. However, the X-ray diffraction patterns of the solids only presented the characteristic peaks of the anatase phase. The catalytic activity of the materials in the photodegradation of Dichlorvos (DDVP) depended on the TiO_2 amount the thermal treatment temperature. The sample containing 30% TiO_2 calcined at 450 °C showed the best catalytic performance and it can be reused without noticeable activity loss during at least four cycles. The catalytic performance was similar to that of the P25 Degussa used as a reference but its separation, recovery and reuse was easier.

1. Introduction

In recent years, advanced oxidation processes (AOPs) have been proposed as innovative water treatment technologies. The rationale of these AOPs is based on the in situ generation of active species (i.e. H_2O_2, OH°, $O_2^{\circ-}$, O_3) for the mineralization of refractory organic compounds, water pathogens and disinfection by-products [1,2]. One of the most widely used processes is heterogeneous photocatalysis, which is the acceleration of a photoreaction by a

* Corresponding author. Tel.: +54 351 469 0585; fax: +54 351 469 0585.
** Corresponding author. Tel.: +54 221 421 1353; fax: +54 221 421 1353.
E-mail addresses: lrpizzio@quimica.unlp.edu.ar, lpierella@gmail.com (L. Pizzio), lpierella@scdt.frc.utn.edu.ar (L. Pierella).

0304-3894/$ – see front matter © 2013 Elsevier B.V. All rights reserved.
http://dx.doi.org/10.1016/j.jhazmat.2013.04.030

catalyst, an attractive and efficient method for the degradation of environmental pollutants or nonbiodegradable toxics present in aqueous domestic, industrial or agricultural effluents.

Titanium dioxide (TiO_2) is one of the most appropriate semiconductor materials to be employed as a photocatalyst, due to its high activity in the photodegradation of organic compounds, low cost, low toxicity, and chemical stability [3,4]. For most photocatalytic reaction systems it is generally accepted that the anatase phase has higher activity than rutile, and this enhancement in photoactivity has been ascribed to the higher Fermi level of anatase than that of rutile by about 0.1 eV [5].

However, there are certain limitations to using bulk TiO_2 in photocatalytic reactors, – for example, due to small size (about 4–30 nm) TiO_2 aggregates in a suspension that rapidly lose their effective surface area as well as their catalytic efficiency. Being nonporous, TiO_2 exhibits low adsorption ability for the pollutants, especially for the nonpolar organic compounds due to their polar surface [6].

The technical limitations of this method are the difficult separation of the catalyst, its reuse and low quantum efficiency [7].

To solve this, recent research has focused on different kinds of supports for dispersing titania catalysts, such as silica [8–10], alumina [11,12], activated carbon [13–15], clay and zeolites [10–12,16,17]. TiO_2 supported on an adsorbent provides higher specific surface area and facilitates more effective adsorption sites than bulk TiO_2 [8,13,16–18]. Recent research, has proposed the synthesis of a zeolite-supported Fe^{3+}-TiO_2 photocatalyst as an alternative to degrade dyes [19].

Zeolites have been investigated as potential supports for photocatalytic systems. They offer several distinct advantages over the other supports such as:

- They have cages and channels of the order of 4–14 Å that can confine substrate molecules to enhance the photocatalytic reactivity. TiO_2 can thus be supported on this zeolite matrix.
- Zeolites behave as electron donors and acceptors of moderate strength toward the guest species depending on the adsorption site [20].

Organophosphorous pesticides are comprised within the 10 most widely used pesticides all over the world. They have been used as an alternative to organochlorine compounds for pest control. However, they are considered as extremely toxic compounds acting on acetylcholinesterase [21]. Their presence as contaminants in aquatic environments may cause serious problems to human beings and other organisms. Dichlorvos (DDVP), an organophosphorous insecticide, is widely used for crop protection mainly in greenhouses and for controlling parasites and insects in houses, aircraft, and outdoor areas (as aerosols, liquid sprays) [22].

In the present work, we report for first time the synthesis of TiO_2 supported on HZSM-11 a medium pore size zeolite with high thermal and chemical resistance. The resulting TiO_2/ZSM-11 materials were characterized by a series of complementary techniques: X-ray diffraction (XRD), ultraviolet–visible diffuse reflectance spectroscopy (DRS), transmittance Fourier transform infrared spectroscopy (FTIR) and scanning electron microscopy (SEM). The materials were evaluated in the photodecomposition of the organophosphate pesticide dichlorvos.

2. Experimental

2.1. Materials

The ZSM-11 zeolite was prepared using the following reactants: sodium aluminate ($NaAlO_2$, Johnson Matthey Electronics), tetrabutylammonium hydroxide (TBAOH, Fluka), Silicic Anhydride (Fluka) and distilled water. For the supported catalysts, titanium (IV) isopropoxide (Aldrich chemistry, 97%) and ethanol (Cicarelli) were employed. P-25, standard TiO_2, was kindly supplied by Degussa. Dichlorvos (Pestanal, Fluka) was selected as the target organic pollutant.

2.2. Preparation of HZSM-11-supported TiO_2 catalyst

The parent Na-ZSM-11 zeolite (Si/Al = 17) was obtained by known methods of hydrothermal crystallization, using TBAOH as a structure directing agent [23]. The ammonium form of the zeolite (NH_4-zeolite) was prepared by ion exchange of the as-prepared Na-zeolite form with 1 M ammonium chloride solution at 80 °C for 40 h. Finally, NH_4-zeolite was dried at 110 °C, treated in a nitrogen flow at 500 °C for 8 h and then calcined in air at the same temperature for 10 h to obtain the HZSM-11 zeolite. The supported catalysts were prepared by taking an appropriate amount of titanium (IV) isopropoxide and zeolite in ethanol, which was mechanically stirred for 4 h at ambient temperature. Then the solvent was removed by rotary evaporation. The amount of titanium (IV) isopropoxide was varied with the purpose of generate in situ TiO_2 concentrations of 3, 10, 20, 30 and 50 wt% in the final solid, and they were denominated TiO_2/HZSM-11(3%), TiO_2/HZSM-11(10%), TiO_2/HZSM-11(20%), TiO_2/HZSM-11(30%) and TiO_2/HZSM-11(50%), respectively. The mixture was then dried at 110 °C and calcined in air at 450 °C. The catalyst TiO_2/HZSM-11(30%) was also calcined at 600 and 800 °C.

In order to compare the activity with the TiO_2/HZSM-11(30%), a physical mixture of P25/HZSM-11(30/70 wt%) was prepared. This mixture was calcined at 450 °C for 8 h.

2.3. Characterization

The powder XRD diffraction patterns of the materials were collected on a PANalytical X'pert PRO diffractometer equipped with Cu Kα (1.54 Å) in the range of 2θ from 5° to 60° in steps of 0.05° with a count time of 2 s at each point. The mean crystallite size (d) of the corresponding phase was estimated using the Scherrer equation and silicon as standard for the correction of the instrumental broadening. It is worth noting that the Scherrer equation was used in order to perform a rough estimation of the crystallite size. BET surface area determinations were carried out with Micromeritics ASAP 2000 equipment. Infrared (IR) studies of TiO_2/zeolites were performed on a JASCO 5300 FTIR spectrometer. The spectra in the lattice vibration region were performed using KBr 0.05% wafer technique and they were carried out from 1800 to 400 cm^{-1} in 16 consecutive registers of 4 cm^{-1} resolution each. The morphological features of supported and unsupported catalysts were obtained using scanning electron microscopy (SEM, FEG-SEM Zeiss Sigma) using fine catalyst powder supported on carbon tape and coated with platinum. UV–vis diffuse reflectance spectra (UV–vis DRS) in absorbance mode were recorded using an Optronics OL 750-427 spectrometer in the wavelength range of 200–900 nm.

Ti, Si and Al content were determined by Inductively Coupled Plasma Optical Emission Spectroscopy (ICP-OES) using a VARIAN, model VISTA MPX – CCD simultaneous ICP-OES. They are provided as supplementary material (Table S1).

2.4. Photocatalytic experiments

The photocatalytic degradation of DDVP was performed in aqueous medium in a batch reactor. A cylindrical Pyrex glass photochemical reactor of 18 cm × 8 cm (height × diameter), provided with water circulation arrangement to maintain the temperature in the range 25–30 °C, was used in all the experiments. The irradiation was carried out using 125 W high-pressure mercury lamp

(with a maximum emission at about 365 nm) placed inside a Pyrex glass jacket, thermostated by water circulation, and immersed in the pesticide solution contained in the batch reactor. The catalyst was maintained in suspension by stirring, and air was continuously bubbled. Previously, the DDVP solution (400 mL, 1×10^{-4} mol/L) containing 100 mg of catalyst was magnetically stirred in the absence of light for 30 min. Aliquots were withdrawn at specific time intervals and analyzed after filtration to remove the catalyst. The variation of the pesticide concentration as a function of irradiation time was determined using a UV-visible Shimadzu spectrophotometer of double beam, measuring the absorbance at 210 nm [24]. In some cases, an HPLC Perkin Elmer with a reverse phase column of C18 measuring 250 mm × 4.6 mm and a mixture of water (50%) with acetonitrile (50%) as solvent at a flow rate of 1 mL min^{-1} was employed. An ion chromatograph (Metrohm – 761 compact IC) equipped with an electroconductivity detector for measuring the phosphate ion formation, was employed. Additionally, a chloride electrode (Phoenix Clo 1508-003B) was used to follow the amount of chloride ions released.

3. Results and discussion

3.1. Characterization of TiO_2/H-zeolite catalysts

3.1.1. XRD analysis

In order to confirm the structure and crystallinity of TiO_2/zeolite catalysts, an XRD study was carried out. Fig. 1 shows the XRD patterns of HZSM-11 (a) and different titania-supported catalysts (b–f). For comparative purposes, the diffraction pattern of commercial P-25 titania (g) is also included. The figure shows the characteristic signal of the parent HZSM-11 catalyst at 2θ angles of 23–24° and 7–9°, which were assigned to (3 3 2), (3 0 3) and (1 0 1), (2 0 0) planes respectively [25]. The XRD pattern of TiO_2/H-ZSM-11(3%) catalyst (Fig. 1(b)) was essentially the same as that of the original HZSM-11 (Fig. 1(a)). TiO_2/HZSM-11 prepared in this study showed diffraction peaks at 25.4°, 48.2°, 54.9° and 55.4°, which were assigned to the characteristic reflections from (1 0 1), (2 0 0), (2 1 1) and (1 0 6) planes of anatase, respectively [5]. In the diffraction pattern of TiO_2/HZSM-11(10%), the peak at (1 0 1) is barely observed, but the other three peaks are not clearly observed since the amount of TiO_2 would not be enough to give clear diffraction peaks.

The peak intensity at 2θ = 25.4° increased with an increasing amount of TiO_2 loaded on HZSM-11. A similar XRD pattern was

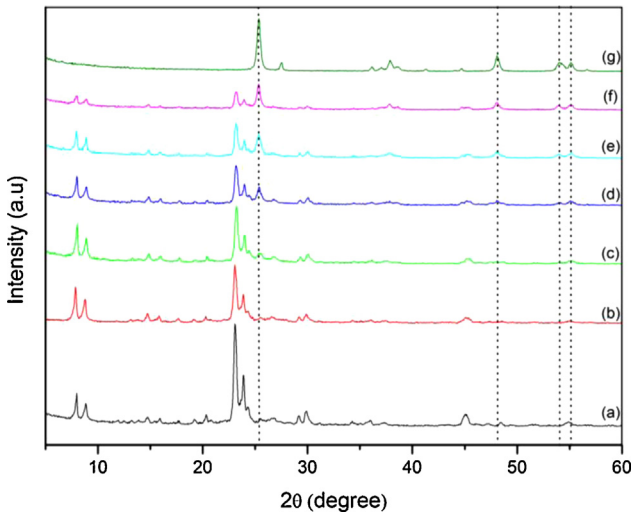

Fig. 1. XRD pattern of (a) zeolite HZSM-11, (b) TiO_2/HZSM-11(3%), (c) TiO_2/HZSM-11(10%), (d) TiO_2/HZSM-11(20%), (e) TiO_2/HZSM-11(30%), (f) TiO_2/HZSM-11(50%) and (g) P-25 Degussa.

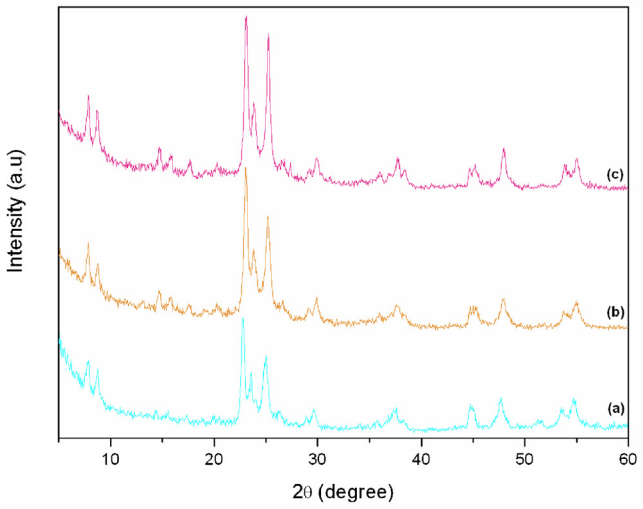

Fig. 2. XRD pattern of TiO_2/HZSM-11(30%) calcined at: (a) 450 °C, (b) 600 °C and (c) 800 °C.

obtained for TiO_2/zeolites (Y, A and BEA), as reported previously [3,26–28]. Simultaneously with the increase in the TiO_2 load, a small decrease in the intensity of HZSM-11 diffraction peaks was observed. However, this decrease can be attributed to a dilution effect of the zeolite matrix in the catalyst.

On the other hand, no peak assigned to rutile phase (2θ = 27.4°) was observed in the XRD patterns of all TiO_2/HZSM-11 catalysts used in the present study.

The calcination temperature effect on TiO_2/zeolite photocatalysts is shown in Fig. 2. The diffraction patterns of the materials did not show the presence of rutile phase, whereas the anatase phase was the phase solely observed whatever the calcination temperatures used. Therefore, it can be suggested that the anatase particles are favorably stabilized on the surface of the zeolite matrix.

The calcination temperature profoundly influenced the crystallite size of TiO_2. As a result of the increment of the calcination temperature from 450 to 800 °C an increase in the size of the anatase crystals was observed. It can be seen in Fig. 2 that the XRD peaks become gradually sharper with increasing temperature, indicating the crystals grew larger in size [5,29] (Table 1).

3.1.2. FTIR spectra

Fig. 3 shows the FTIR spectra of bulk TiO_2, bulk zeolite and TiO_2/HZSM-11 (wt%) in the range of 1800–400 cm^{-1}. All the zeolitic materials present vibrations assigned to the internal bonds of a TO_4 tetrahedral structure (T = Si or Al) that are insensitive to changes in the zeolite structure, 1250–950, 850–700 cm^{-1} and the signals at 500–420 cm^{-1} being attributed to asymmetrical stretching, to the symmetrical stretching and to (O—T—O) deformation, respectively. Furthermore, vibrations assigned to the external bonds of the TO_4 tetrahedral structure, which are sensitive to changes in the structure, can also be observed. These vibrations, in the region between 650 and 500 cm^{-1}, are attributed to those of double rings consisting of five atoms. A shoulder between 1050 and 950 cm^{-1} is assigned to the asymmetrical stretching of T—O—T bonds [30].

No band in the region near 960 cm^{-1} was detected, which could be assigned to the antisymmetric stretching vibration of the

Table 1
Crystallite size of TiO_2 in the zeolite.

Sample	*d* (nm)
TiO_2/HZSM-11(30%)-450 °C	10
TiO_2/HZSM-11(30%)-600 °C	12.5
TiO_2/HZSM-11(30%)-800 °C	16.7

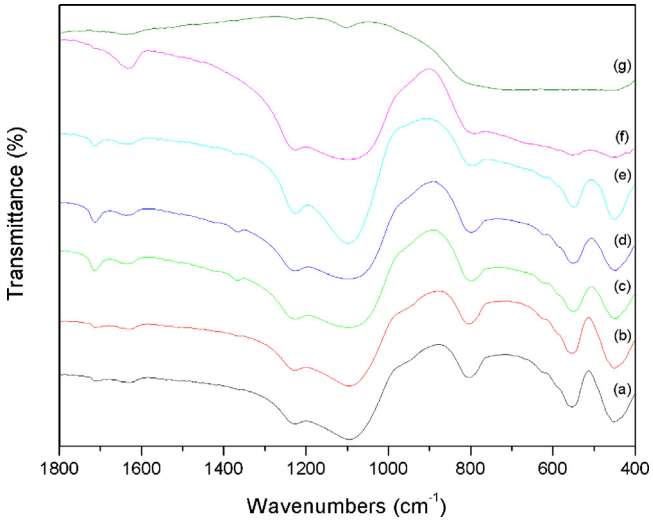

Fig. 3. FTIR of (a) zeolite HZSM-11, (b) TiO_2/HZSM-11(3%), (c) TiO_2/HZSM-11(10%), (d) TiO_2/HZSM-11(20%), (e) TiO_2/HZSM-11(30%), (f) TiO_2/HZSM-11(50%) and (g) P-25 Degussa.

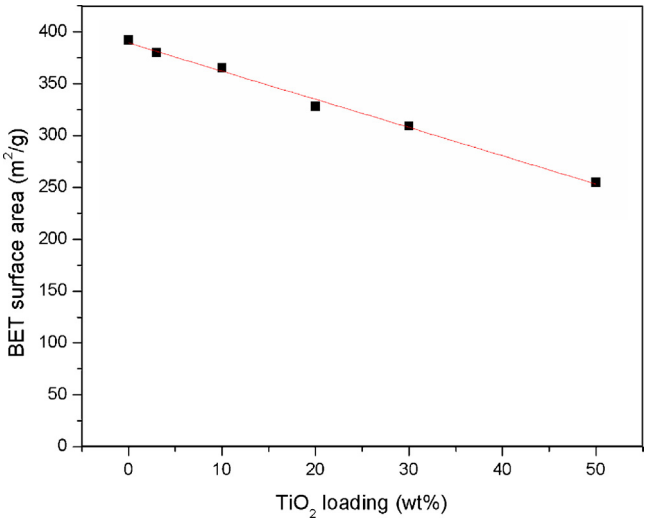

Fig. 4. BET surface area versus TiO_2 loading (wt%) over the zeolite matrix.

Ti—O—Si bonds [28,31,32]. Therefore, the replacement of the tetrahedral Si sites with Ti during preparation did not take place. So, we can conclude that TiO_2 was deposited on the surface of the zeolites.

3.1.3. BET surface area

The surface area (S_{BET}) of the synthesized materials was determined from the N_2 adsorption–desorption isotherms using the Brunauer–Emmett–Teller method. The adsorption–desorption isotherms of TiO_2/HZSM-11 samples exhibit characteristics similar to those of HZSM-11. According to IUPAC classification, they are Type I isotherms, characteristic of microporous solids having relatively small external surfaces [33].

With increasing loading of TiO_2, a linear decrease in the surface area (S_{BET}) of the samples can be seen (Fig. 4). This could be due to deposition of TiO_2 particles on the HZSM-11 surface and blocking of the pores.

On the other hand, the S_{BET} of the samples TiO_2/HZSM-11(30%) calcined at different temperatures decreases when the calcination temperature increases. For the 450 °C, 600 °C and 800 °C samples, the surface area were 309, 296, 293 m^2/g, respectively. This could be explained by the TiO_2 agglomeration/growth phenomena during the calcination treatments.

3.1.4. SEM

The morphology of the zeolitic supports and the supported catalysts was studied using SEM. According to the SEM images (Fig. 5) the zeolite matrix presents prismatoid-like crystals. The surface morphology of the TiO_2/HZSM-11(30%) sample shows the prismatoid crystals characteristic of zeolite and TiO_2 spherical nanoparticles (size in the range 200–400 nm) and clusters attached to the zeolite surface.

3.1.5. UV–vis DRS

The UV–vis diffuse reflectance spectra of zeolite matrix and TiO_2/HZSM-11 samples are shown in Fig. 6. The diffuse reflectance spectrum of HZSM-11 (Fig. 6(a)) consists of a single band at 210 nm arising from the Al—O charge-transfer transition of four-coordinated framework aluminum, characteristic of as-synthesized zeolites [34]. In the supported catalyst, the absorption band at 200–250 nm is due to electron transfer from the ligand–oxygen to an unoccupied orbital of the Ti^{4+} framework [35]. The spectra are also characterized by an intense band centered at 320 nm, corresponding to charge transfer from the valence band (O 2p) to the conduction band (Ti 3d) [36].

The determination of the band gap from the UV–vis spectra is an alternative method to study the modification of the electronic properties of the TiO_2 species [34]. The band gap of TiO_2 can be affected by the particle size (quantum size effects) and the particle size could be affected by the thermal treatment temperature and of TiO_2 contents among others for TiO_2 hybrid systems [37–39]. The band gap energies were estimated from UV–vis-DRS spectra using the Kubelka–Munk remission function [29]. The estimated E_g values for the different samples are listed in Table 2. The UV–vis-DRS spectra of the TiO_2/HZSM-11 samples showed the absorption threshold onset was scarcely shifted to the visible region when

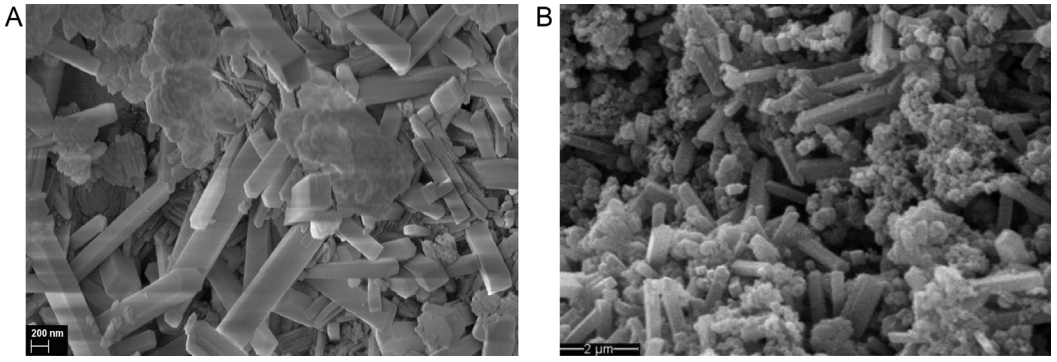

Fig. 5. SEM images of (A) zeolite HZSM-11 and (B) TiO_2/HZSM-11(30%).

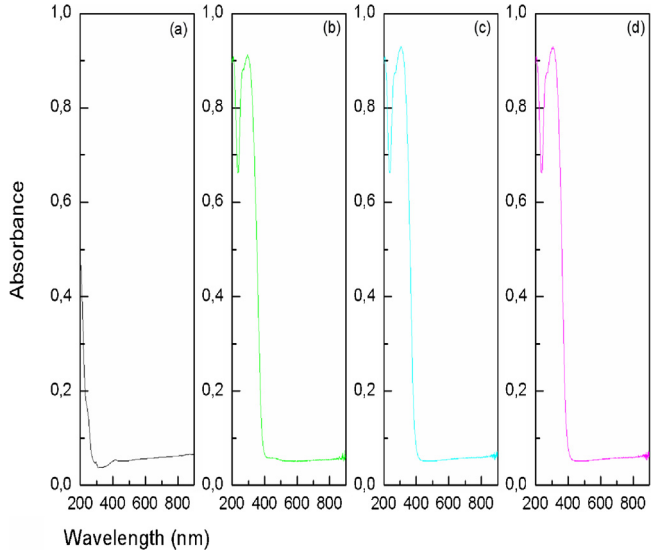

Fig. 6. DRS of (a) zeolite HZSM-11, (b) TiO_2/HZSM-11(10%), (c) TiO_2/HZSM-11(30%) and (d) TiO_2/HZSM-11(50%).

Table 2
E_g values for the supported catalyst.

Sample	Band gap (eV)[a]
TiO_2/HZSM-11(10%)	3.25
TiO_2/HZSM-11(30%)	3.15
TiO_2/HZSM-11(50%)	3.12

[a] ±0.5 eV.

the TiO_2 concentration increased. As result, the E_g values present a small variation when varying TiO_2 content in the samples.

3.2. Photocatalytic evaluation

3.2.1. Primary studies

Prior to photocatalytic experiments, the DDVP solution (400 mL, 1×10^{-4} mol/L) with 100 mg of catalyst (HZSM-11 or TiO_2/HZMS-11 (wt%) samples) was magnetically stirred in the absence of light to study the adsorption on the surface of the materials. The maximum adsorption was reached after 30 min. These results show that at least 30 min are necessary to the attainment of the adsorption–desorption equilibrium of DDVP on the surface of the materials.

The results of the photolysis experiments carried out without any catalyst are depicted in Fig. 7(A). During the reaction it was observed that only 2–5% degradation occurred. In the presence of HZSM-11 as catalyst, no significant degradation was observed confirming that HZMS-11 is not active by itself in the degradation of DDVP.

3.2.2. Effect of TiO_2 content on TiO_2/HZSM-11 samples

The effect of TiO_2 percentage on the HZSM-11 in the photocatalytic activity is shown in Fig. 7(A) and (B). The studies were made using 100 mg of catalyst in 400 mL of DDVP aqueous solution. The degradation percentage was calculated as $X = (C_0 - C/C_0) \times 100$, where C_0 is the original DDVP concentration and C the remaining DDVP concentration in solution at specific time intervals. As can be seen, the increment of TiO_2 content in TiO_2/HZSM-11 samples from 3 to 30 wt% produces a continuous increment of the photocatalytic activity. The decline in the degradation of samples with loadings higher than TiO_2/HZSM-11(30%), could be due to the presence of TiO_2 particle aggregates of higher size on the zeolite matrix surface.

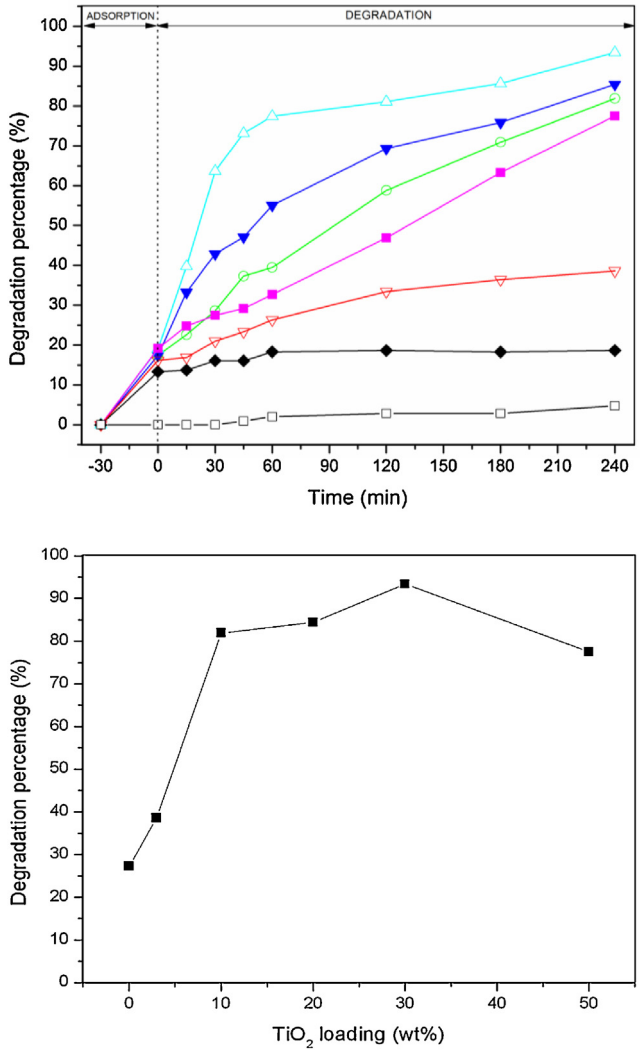

Fig. 7. Effect of TiO_2 content on HZSM-11 (A) (□) photolysis (♦) HZSM-11 (▽) TiO_2/HZSM-11(3%), (○) TiO_2/HZSM-11(10%) (▼) TiO_2/HZSM-11(20%), (△) TiO_2/HZSM-11(30%) and (■) TiO_2/HZSM-11(50%). (B) Percentage of degradation at the end of the reaction versus TiO_2 loading (wt%). Experimental conditions: $[DDVP]_{initial}$: 1×10^{-4} mol/L; pH: 5 and catalyst/solution ratio equal to 250 mg/L.

The catalyst with the best performance in the DDVP degradation (TiO_2/HZSM-11(30%)) was chosen for further studies.

The DDVP degradation was monitored following the mineralization products Cl^- and PO_4^{3-} anions as a function of the irradiation time (Fig. 8).

After 240 min of irradiation the amount of DDVP degraded was close to 90%. It can be observed that at the same irradiation time, the ratio between the amount of Cl^- anions released and the amount of DDVP molecules degraded is close to 2. These results are in agreement with previous reports that indicate that the cleavage of the Cl-aryl bond releases inorganic chloride to the reacting medium [21].

On the other hand, the amount of PO_4^{3-} anions released was only 15% of the total amount of phosphate present in the original DDVP solution, which indicates the formation of phosphate-containing intermediates [40]. The total mineralization of the pollutant was not obtained under these conditions. According Shifu and Gengyu [41] the intermediate products formed during the photocatalytic degradation of dichlorvos are trimethyl phosphate, formic acid and acetic acid. Trimethyl phosphate has been identified as an intermediate of the photocatalytic oxidation of

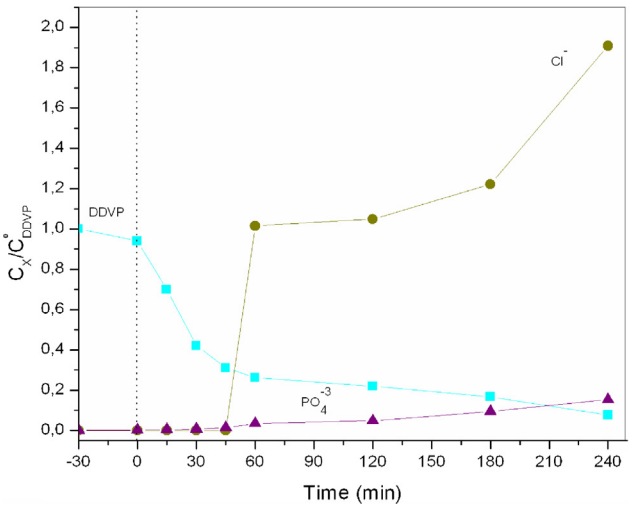

Fig. 8. DDVP degradation and Cl^-, PO_4^{3-} release employing TiO_2/HZSM-11(30%). C_x is the actual concentration of: DDVP, PO_4^{3-} or Cl^-. C°_{DDVP} is the initial concentration the DDVP.

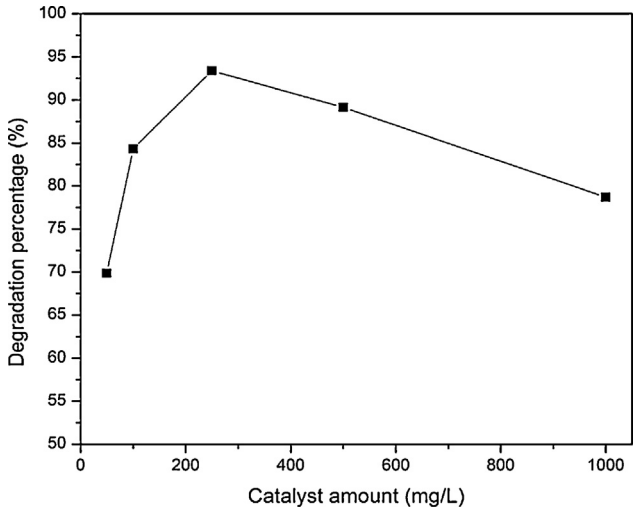

Fig. 10. Effect of TiO_2/HZSM-11(30%) catalyst amount on DDVP degradation. Experimental conditions: $[DDVP]_{initial}$: 1×10^{-4} mol/L and pH: 5.

dichlorvos elsewhere. This compound appears to be less toxic than the parent compound [21].

3.2.3. Effect of catalyst preparation

According to Chatti et al. [20], the TiO_2 incorporation mode played an important role in the photocatalytic activity of the synthesized photocatalysts. Fig. 9 shows the catalytic activity of TiO_2/HZSM-11(30%) and a physical mixture of TiO_2 and HZSM-11 containing the same amount of titania as that of the sample prepared by the impregnation method.

We can see that the catalyst synthesized using titanium isopropoxide (as titanium source) shows the best photocatalytic activity. This may be attributed to better dispersion and interaction of TiO_2 particles over the zeolite matrix.

On the other hand, to understand the role of the support (i.e., beneficial or detrimental effect) during the photocatalytic degradation, comparative studies between TiO_2/HZSM-11(30%) (obtained by the impregnation method) and bulk TiO_2 (Degussa P25) were carried out. Fig. 9 shows similar degradation of the TiO_2-supported system compared to bulk TiO_2. Finally, at 240 min

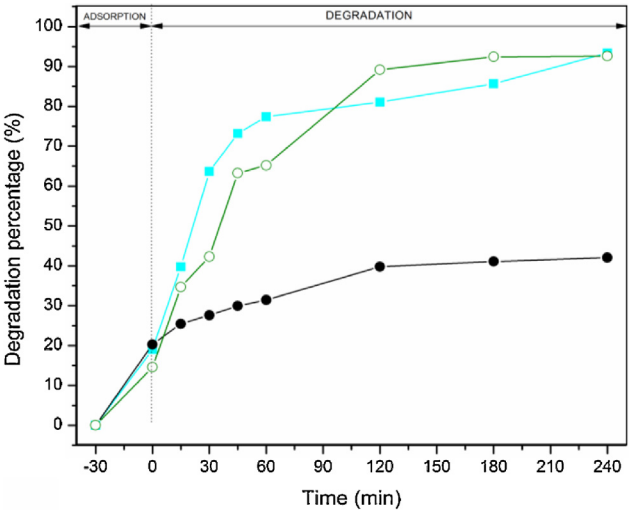

Fig. 9. Comparative photocatalyst performance (●) physical mixture (■) impregnation (○) P25 TiO_2. Experimental conditions: $[DDVP]_{initial}$: 1×10^{-4} mol/L; pH: 5 and catalyst/solution ratio equal to 250 mg/L.

both materials reach almost the same degradation. This may be caused by the synergistic effect resulting from the adsorption of DDVP on the material. This can facilitate the degradation without affecting the photocatalytic properties of TiO_2. The delocalization of electrons at the support material and the adsorption properties of the support enhance the degradation [7]. Also, the dispersion of TiO_2 over zeolite material avoids particle–particle aggregation and light scattering by TiO_2. The good dispersion leads to the presence of more holes available near the adsorbed DDVP molecules resulting in faster degradation rates.

3.2.4. Effect of catalyst content

The effect of catalyst concentration on the degradation of DDVP was investigated employing different concentrations of catalyst TiO_2/HZSM-11(30%), in the range 50–1000 mg/L, keeping all other experimental parameters constant (Fig. 10). The DDVP degradation increases with the increment of the catalyst concentration from 50 to 250 mg/L. However, further increments in catalyst concentration lead to a continuous decrease of the DDVP degraded amount. When the TiO_2/HZSM-11(30%) concentration is high (above 250 mg/L), a screening effect is produced. The degradation diminishes due to the excessive opacity of the suspension, which prevents the catalyst farthest in from being illuminated [24]. Further, at a higher catalyst amount it is difficult to maintain the suspension homogeneous due to particle agglomeration, which decreases the number of active sites [27].

3.2.5. Effect of catalyst calcination temperature

The photodegradation efficiency of TiO_2/HZSM-11(30%) decreased with the increment of the calcination temperature from 93 to 86% for samples calcined between 450 and 800 °C respectively. The slight decrease of DDVP degradation percentage could be due to the increment of TiO_2 crystal size and the sinter of TiO_2 particles. As above-mentioned in the XRD analysis, higher calcination temperatures produce larger TiO_2 crystallites over the zeolite surface.

3.2.6. Effect of initial pH value

According to Mahalakshmi et al. [27], the solution pH is an important variable in aqueous phase mediated photocatalytic reactions. The pH solution influences the adsorption and dissociation of the substrate, the catalyst surface charge, the oxidation potential of the valence band and other physicochemical properties of the system [27]. The effect of pH on the photocatalytic degradation was

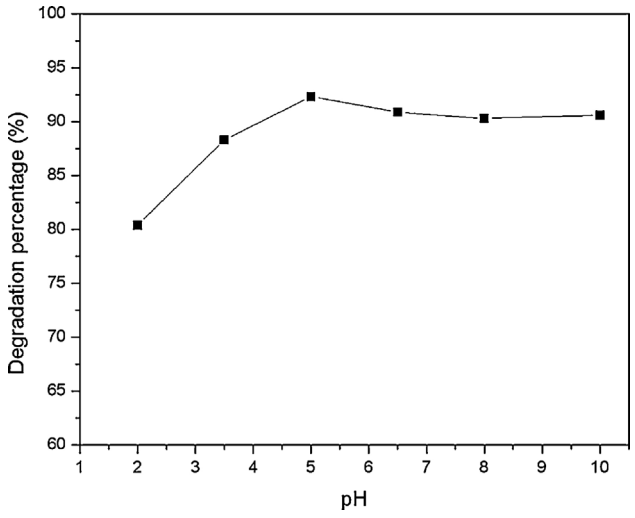

Fig. 11. Effect of pH on DDVP degradation. Experimental conditions: $[DDVP]_{initial}$: 1×10^{-4} mol/L, catalyst: TiO_2/HZSM-11(30%) and catalyst/solution ratio equal to 250 mg/L.

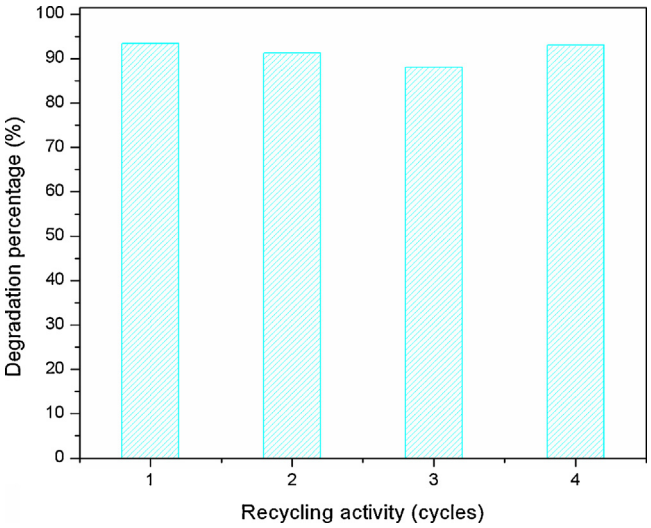

Fig. 12. DDVP degradation degree as a function of the number cycle for the TiO_2/HZSM-11(30%) catalyst. Experimental conditions: $[DDVP]_{initial}$: 1×10^{-4} mol/L; pH: 5 and catalyst/solution ratio equal to 250 mg/L.

studied by varying the initial pH of the DDVP solution and keeping all other experimental conditions constant.

The initial solution pH in the reactions evaluated in previous paragraphs is 5. In order to compare the standard reaction with the initial pH = 5, some reactions were carried out with initial acid pH and alkaline pH in the range of 2–10, which were adjusted with hydrochloric acid and sodium hydroxide, respectively (Fig. 11). We can see that the DDVP degradation decreases when the pH was in the range 2–4, and remains practically constant when it was in the range 6–10.

The effect of pH on the photocatalytic reaction is generally attributed to the surface charge of TiO_2 and its relation with the ionic form of the organic compound (anionic or cationic). Electrostatic attraction or repulsion between the surface of the catalyst and the organic molecule is taking place and consequently enhances or inhibits, respectively, the photodegradation rate.

Taking into that dichlorvos is an unionizable compound, and according to Evgenidou et al. [40], the decrease of the reaction rate at acid pH can be ascribed to the lower hydroxylation of the catalyst's surface due to the presence of a small amounts of OH^- ions.

3.3. Catalyst recycling study

At the end of the first catalytic cycle, the catalyst was filtered, washed, oven dried at 70 °C and then reused without any calcination treatment. The same procedure was employed after the second cycle of usage. From the comparison of the DDVP degradation degree reached at the end of the 1st the 2nd and the 3rd cycle, a slight decrease in degradation rate was noticed (Fig. 12). The decrease in degradation percentage was probably due to the accumulation of organic intermediates in the cavities and on the surface of the catalyst affecting the adsorption of DDVP, and reducing the activity of the catalytic material. The catalyst recovered after the 3rd cycle was calcined at 450 °C for 8 h and reused. As we can see, the original activity was restored (Fig. 12, 4th cycle).

Hence, calcination of the reused catalyst is necessary in order to regenerate the activity. Furthermore, this is substantiated by comparing the surface characterization studies of fresh and used catalysts (before and after the 4th cycle) with XRD in Fig. 13. The XRD pattern showed that the sample was intact even after the 4th cycle. The characteristic peaks of TiO_2 phase in the used catalyst are the same as those in the fresh sample. Thus, this proves that the

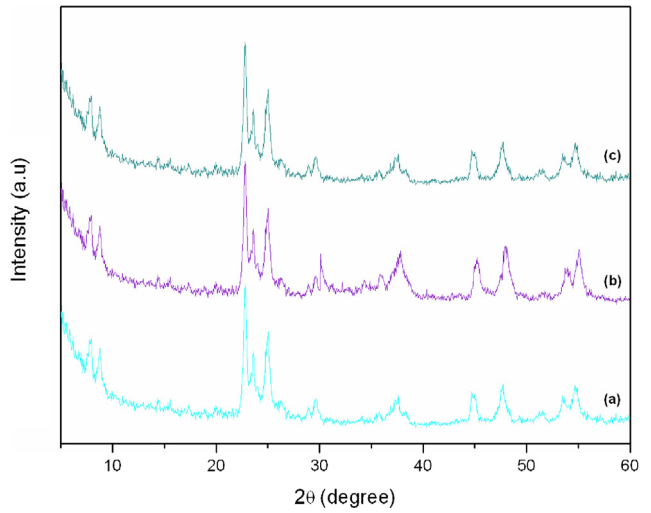

Fig. 13. XRD of TiO_2/HZSM-11(30%). (a) Fresh, (b) used–without regeneration (after cycle 3rd) and (c) used – with calcination (after cycle 4th).

catalyst is highly stable and is reusable for several cycles without losing its original activity.

It is worth noting that no leaching of titanium dioxide from TiO_2/ZSM-11 samples occurs during the reaction. TiO_2 could not be detected in the liquid filtrate after each cycle of usage. Additionally, no significant conversion of dichlorvos was observed when the reaction was carried out dissolving DDVP in the liquid filtrate without TiO_2/HZSM-11(30%) as catalyst. These observations strongly suggest that the reaction proceeds heterogeneously over the catalyst.

4. Conclusions

Catalysts based on titania supported on ZSM-11 zeolite were synthesized by taking an amount of titanium (IV) isopropoxide and of zeolite in ethanol. The diffraction patterns of the materials did not show the presence of rutile phase, whereas the anatase phase was the phase solely observed whatever the calcination temperatures and the TiO_2 content used. It can be suggested that the anatase particles are stabilized on the surface of the zeolite matrix.

The results of the present investigation indicate that the best catalyst was TiO_2/ZSM-11(30%) prepared by the impregnation method. Several variables were studied and it was observed that the best operating conditions were: DDVP solution, pH = 5; calcination temperature of the catalyst, 450 °C; and catalyst/solution ratio equal to 250 mg/L.

After regenerating the materials used no significant changes in the structure and activity were observed, so they can be reused without noticeable activity loss during at least four cycles.

The TiO_2/ZSM-11 catalysts prepared in this study were suitable for the degradation of the insecticide DDVP in water, resulting in degradation percentages similar to the commercial TiO_2 P25. The advantage of supported catalysts, in comparison with the commercial ones, is mainly its easy separation and reuse.

Acknowledgement

This project was partially supported by: Foncyt PICT 2007-00303, Mincyt-Córdoba PID 000121 and PID UTN 25/E129. We thank CONICET: L.B.Pierella, L.R. Pizzio, C. Leal Marchena and S. Gomez.

Appendix A. Supplementary data

Supplementary data associated with this article can be found, in the online version, at http://dx.doi.org/10.1016/j.jhazmat.2013.04.030.

References

[1] M.V. Phanikrishna Sharma, K. Lalitha, V. Durgakumari, M. Subrahmanyam, Solar photocatalytic mineralization of isoproturon over TiO_2/HY composite systems, Sol. Energy Mater. Sol. Cells 92 (2008) 332–342.
[2] M.N. Chong, B. Jin, C.W.K. Chow, C. Saint, Recent developments in photocatalytic water treatment technology: a review, Water Res. 44 (2010) 2997–3027.
[3] S. Yamaguchi, T. Fukura, Y. Imai, H. Yamaura, H. Yahiro, Photocatalytic activities for partial oxidation of methylstyrene over zeolite-supported titanium dioxide and the influence of water addition to reaction solvent, Electrochim. Acta 55 (2009) 7745–7750.
[4] V. Fuchs, L. Méndez, M. Blanco, L. Pizzio, Mesoporous titania directly modified with tungstophosphoric acid: synthesis, characterization and catalytic evaluation, Appl. Catal. A: Gen. 358 (2009) 73–78.
[5] K. Porkodi, S.D. Arokiamary, Synthesis and spectroscopic characterization of nanostructured anatase titania: a photocatalyst, Mater. Charact. 58 (2007) 495–503.
[6] A. Bhattacharyya, S. Kawi, M.B. Ray, Photocatalytic degradation of orange II by TiO_2 catalysts supported on adsorbents, Catal. Today 98 (2004) 431–439.
[7] M.V. Phanikrishna Sharma, V. Durga Kumari, M. Subrahmanyam, TiO_2 supported over SBA-15: an efficient photocatalyst for the pesticide degradation using solar light, Chemosphere 73 (2008) 1562–1569.
[8] C. Anderson, A.J. Bard, An improved photocatalyst of TiO_2/SiO_2 prepared by a sol–gel synthesis, J. Phys. Chem. 99 (1995) 9882–9885.
[9] G.P. Lepore, L. Persaud, C.H. Langford, Supporting titanium dioxide photocatalysts on silica gel and hydrophobically modified silica gel, J. Photochem. Photobiol. A: Chem. 98 (1996) 103–111.
[10] Y. Xu, W. Zheng, W. Liu, Enhanced photocatalytic activity of supported TiO_2: dispersing effect of SiO_2, J. Photochem. Photobiol. A: Chem. 122 (1999) 57–60.
[11] C. Minero, F. Catozzo, E. Pelizzetti, Role of adsorption in photocatalyzed reactions of organic molecules in aqueous TiO_2 suspensions, Langmuir 8 (1992) 481–486.
[12] C. Anderson, A.J. Bard, Improved photocatalytic activity and characterization of mixed TiO_2/SiO_2 and TiO_2/$Al2O_3$ materials, J. Phys. Chem. B 101 (1997) 2611–2616.
[13] T. Torimoto, Y. Okawa, N. Takeda, H. Yoneyama, Effect of activated carbon content in TiO_2-1oaded activated carbon on photodegradetion behaviors of dichloromethane, J. Photochem. Photobiol. A: Chem. 103 (1997) 153–157.
[14] J. Hermann, J. Matos, J. Disdier, C. Guillard, J. Laine, S. Malato, J. Blanco, Solar photocatalytic degradation of 4-chlorophenol using the synergistic effect between titania and activated carbon in aqueous suspension, Catal. Today 54 (1999) 255–265.
[15] H. Yoneyama, T. Torimoto, Titanium dioxide/adsorbent hybrid photocatalysts for photodestruction of organic substances of dilute concentrations, Catal. Today 58 (2000) 133–140.
[16] Y. Xu, C.H. Langford, Enhanced photoactivity of a titanium (1 V) Oxide Supported on ZSMS and zeolite A at low coverage, J. Phys. Chem. 99 (1995) 11501–11507.
[17] Y. Xu, C.H. Langford, Photoactivity of Titanium Dioxide Supported on MCM41, Zeolite X, and Zeolite Y, J. Phys. Chem. B 101 (1997) 3115–3121.
[18] N. Takeda, M. Ohtani, T. Torimoto, S. Kuwabata, H. Yoneyama, Evaluation of diffusibility of adsorbed propionaldehyde on titanium dioxide-loaded adsorbent photocatalyst films from its photodecomposition rate, J. Phys. Chem. 101 (1997) 2644–2649.
[19] C. Wang, H. Shi, Y. Li, Synthesis and characteristics of natural zeolite supported Fe^{3+}-TiO_2 photocatalysts, Appl. Surf. Sci. 257 (2011) 6873–6877.
[20] R. Chatti, S.S. Rayalu, N. Dubey, N. Labhsetwar, S. Devotta, Solar-based photoreduction of methyl orange using zeolite supported photocatalytic materials, Sol. Energy Mater. Sol. Cells 91 (2007) 180–190.
[21] E. Evgenidou, I. Konstantinou, K. Fytianos, T. Albanis, Study of the removal of dichlorvos and dimethoate in a titanium dioxide mediated photocatalytic process through the examination of intermediates and the reaction mechanism, J. Hazard. Mater. B 137 (2006) 1056–1064.
[22] S.A. Naman, Z.A.-A. Khammas, F.M. Hussein, Photo-oxidative degradation of insecticide dichlorovos by a combined semiconductors and organic sensitizers in aqueous media, J. Photochem. Photobiol. A: Chem. 153 (2002) 229–236.
[23] O. Anunziata, L. Pierella, Nature of the active sites in H-ZSM-11 zeolite modified with $Zn^{(2+)}$ and $Ga^{(3+)}$, Catal. Lett. 19 (1993) 143–151.
[24] M. Atiqur Rahman, M. Muneer, Photocatalysed degradation of two selected pesticide derivatives, dichlorvos and phosphamidon, in aqueous suspensions of titanium dioxide, Desalination 181 (2005) 161–172.
[25] M.S. Renzini, U. Sedrán, L.B. Pierella, H-ZSM-11 and Zn-ZSM-11 zeolites and their applications in the catalytic transformation of LDPE, J. Anal. Appl. Pyrolysis 86 (2009) 215–220.
[26] H. Chen, A. Matsumoto, N. Nishimiya, K. Tsutsumi, Preparation and characterization of TiO_2 incorporated Y-zeolite, Colloids Surf. A 157 (1999) 295–305.
[27] M. Mahalakshmi, S. Vishnu Priya, B. Arabindoo, M. Palanichamy, V. Murugesan, Photocatalytic degradation of aqueous propoxur solution using TiO_2 and Hβ zeolite-supported TiO_2, J. Hazard. Mater. 161 (2009) 336–343.
[28] D.I. Petkowicz, R. Brambilla, C. Radtke, C. Silva da Silva, Z.N. da Rocha, S.B.C. Pergher, J.H.Z. dos Santos, Photodegradation of methylene blue by in situ generated titania supported on a NaA zeolite, Appl. Catal. A: Gen. 357 (2009) 125–134.
[29] A.M. Luís, M.C. Neves, M.H. Mendon, O.C. Monteiro, Influence of calcination parameters on the TiO_2 photocatalytic properties, Mater. Chem. Phys. 125 (2011) 20–25.
[30] O.A. Anunziata, A.R. Beltramone, Z. Juric, L.B. Pierella, F.G. Requejo, Fe-containing ZSM-11 zeolites as active catalyst for SCR of NO_x Part I. Synthesis, characterization by XRD, BET and FTIR and catalytic properties, Appl. Catal. A: Gen. 264 (2004) 93–101.
[31] C. Wang, C. Lee, M. Lyu, L. Juang, Photocatalytic degradation of C.I. Basic Violet 10 using TiO_2 catalysts supported by Y zeolite: an investigation of the effects of operational parameters, Dyes Pigments 76 (2008) 817–824.
[32] Y. Kim, M. Yoon, TiO_2/Y-Zeolite encapsulating intramolecular charge transfer molecules: a new photocatalyst for photoreduction of methyl orange in aqueous medium, J. Mol. Catal. A: Chem. 168 (2001) 257–263.
[33] K.S.W. Sing, D.H. Everett, R.A.W. Haul, L. Moscou, R.A. Pierotti, J. Rouquerol, T. Siemieniewska, Reporting physisorption data for gas/solid systems: with special reference to the determination of surface area and porosity, Pure Appl. Chem. 57 (4) (1985) 603–619, IUPAC.
[34] M.A. Zanjanchi, A. Razavi, Identification and estimation of extra-framework aluminium in acidic mazzite by diffuse reflectance spectroscopy, Spectrochim. Acta A 57 (2001) 119–127.
[35] D.I. Petkowicz, S.B.C. Pergher, C.D. Silva da Silva, Z.N. da Rocha, J.H.Z. dos Santos, Catalytic photodegradation of dyes by in situ zeolite supported titania, Chem. Eng. J. 158 (2010) 505–512.
[36] J. Liqiang, S. Xiaojun, C. Weimin, X. Zili, D. Yaoguo, F. Honggang, The preparation and characterization of nanoparticle of TiO_2/Ti films and their photocatalytic activity, J. Phys. Chem. Solids 64 (2003) 615–623.
[37] L. Kavan, T. Stoto, M. Gratzel, Quantum size effects in nanocrystalline semiconducting TiO_2 layers prepared by anodic oxidative hydrolysis of $TiC1_3$, J. Phys. Chem. 97 (1993) 9493–9498.
[38] Y. Li, T.J. White, S.H. Lim, Low-temperature synthesis and microstructural control of titania nano-particles, J. Solid State Chem. 177 (2004) 1372–1381.
[39] T. Ohno, S. Tagawa, H. Itoh, H. Suzuki, T. Matsuda, Size effect of TiO_2–SiO_2 nanohybrid particle, Mater. Chem. Phys. 113 (2009) 119–123.
[40] E. Evgenidou, K. Fytianos, I. Poulios, Semiconductor-sensitized photodegradation of dichlorvos in water using TiO_2 and ZnO as catalysts, Appl. Catal. B: Environ. 59 (2005) 81–89.
[41] C. Shifu, C. Gengyu, Photocatalytic degradation of organophosphorus pesticides using floating photocatalyst TiO_2·SiO_2/beads by sunlight, Solar Energy 79 (2005) 1–9.